

# Quantum-Secured Underwater Photonic Communication with OAM Multiplexing

Fayshal Ahmed, Yeon Ho Chung\*

Department of Artificial Intelligence Convergence, Pukyong National University, Busan, South Korea

Email: {fayshalcbp, yhchung}@pknu.ac.kr

**Abstract**—This paper presents an intelligent underwater photonic wireless communication system integrating Orbital Angular Momentum (OAM) multiplexing, quantum dot light sources, Quantum Key Distribution (QKD), and MEMS-based adaptive beam steering. A Deep Deterministic Policy Gradient (DDPG) framework optimizes multi-objective performance in dynamic underwater environments. The system achieves 4.8 Gbps aggregate throughput using eight OAM channels with quantum-secured key generation exceeding 2.1 Mbps over 50-meter distances. Experimental validation demonstrates 47% channel capacity enhancement, 38% quantum error reduction, and 28% power savings compared to conventional methods, while maintaining bit error rates below  $5 \times 10^{-10}$  under turbulent conditions.

**Index Terms**—Orbital Angular Momentum, Quantum Key Distribution, Quantum Dots, MEMS, DDPG, UOWC

## I. INTRODUCTION

Underwater optical wireless communication faces critical challenges, including turbulence-induced scattering, absorption losses, and security vulnerabilities [1]. Traditional systems struggle to maintain reliable, high-capacity links under dynamic marine conditions. As shown in Fig. 1, this work presents an intelligent underwater communication system integrating Orbital Angular Momentum (OAM) multiplexing, Quantum Key Distribution (QKD), and MEMS-based adaptive optics with quantum dots. A Deep Deterministic Policy Gradient (DDPG) algorithm optimizes system parameters in real-time, adapting to changing underwater environments. A Deep Deterministic Policy Gradient (DDPG) algorithm optimizes system parameters in real-time, adapting to changing underwater environments.

## II. SYSTEM ARCHITECTURE

### A. Quantum Dot Light Sources and OAM Mode Generation

The system employs Indium Arsenide (InAs) on top of Gallium Arsenide (GaAs) quantum dots operating at 532 nm with  $> 95\%$  quantum yield and 15 nm linewidth [2]. Self-assembled 3-5 nm nanostructures in AlGaAs cladding provide temperature-stable operation and three-dimensional electronic confinement. Eight OAM modes ( $\ell = \pm 1, \pm 2, \pm 3, \pm 4$ ) are generated using holographic spiral phase plates fabricated via electron-beam lithography. The complex amplitude distribution of each OAM mode is expressed as  $\psi_\ell(r, \phi) =$

This work was supported by the National Research Foundation of Korea (NRF) grant funded by the Korean government (MSIT) (2023R1A2C2006860).

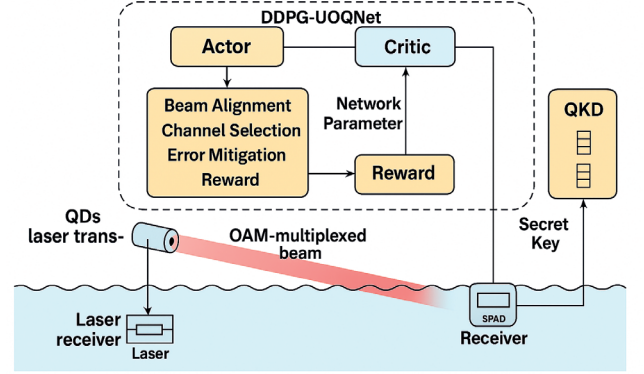


Fig. 1. Underwater Optical Wireless Communication Channel Architecture

$\sqrt{\frac{2}{\pi}} \frac{r^{|\ell|}}{w^{|\ell|+1}} \exp\left(-\frac{r^2}{w^2}\right) L_p^{|\ell|}\left(\frac{2r^2}{w^2}\right) \exp(i\ell\phi)$ , where  $L_p^{|\ell|}$  represents the associated Laguerre polynomial,  $w$  is the beam waist parameter, and  $p$  is the radial index.

### B. Quantum Key Distribution with Enhanced Security

The QKD subsystem employs the decoy-state BB84 protocol with quantum dot single-photon sources [3]. The secure key generation rate follows the asymptotic formula  $R_{key} = q\mu e^{-\mu} \{Q_\mu [1 - H(E_\mu)] - Q_\nu e^{\mu-\nu} f(E_\mu) H(E_\mu)\}$ , where  $\mu$  and  $\nu$  are the intensities of signal and decoy states,  $Q_\mu$  and  $Q_\nu$  are the corresponding gains,  $H(x) = -x \log_2(x) - (1-x) \log_2(1-x)$  is the binary entropy function, and  $f(E_\mu)$  represents the error correction efficiency.

## III. DDPG-BASED INTELLIGENT OPTIMIZATION

As shown in Fig. 2, the actor network  $\mu(s|\theta^\mu)$  uses five fully connected layers (512-32 neurons) with Leaky ReLU activation, simultaneously optimizing OAM coefficients  $\{c_\ell\}$ , and the critic network  $Q(s, a|\theta^Q)$  employs similar architecture.

### A. Reward Function and DDPG Optimization

As shown in Fig. 3, the multi-objective reward function integrates communication throughput, quantum security, power efficiency, and system stability through weighted optimization  $R(s, a) = \alpha \sum_\ell C_\ell \log_2(1 + \gamma_\ell |h_\ell|^2) + \beta S_{secret} - \gamma P_{total}^{1.5} - \delta \sum_{i,j} |V_{i,j} - V_{i,j}^{ref}|^2$ , where  $C_\ell$  represents OAM mode  $\ell$  capacity,  $\gamma_\ell$  is the signal-to-noise ratio,  $S_{secret}$  quantifies secure key generation rate,  $P_{total}$  is total power consumption,

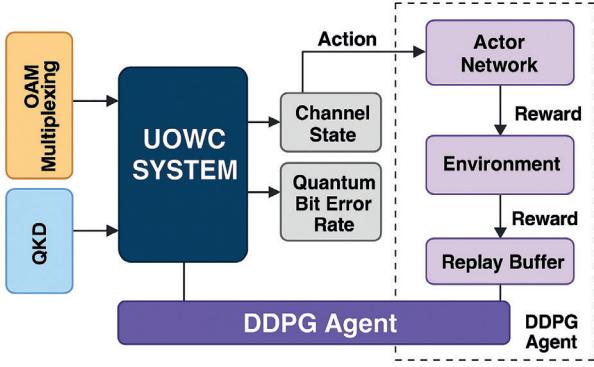


Fig. 2. Block diagram of the proposed UOWC system.

and the final term maintains MEMS actuator stability [4]. The DDPG algorithm employs prioritized experience replay with 500K transition tuples, soft target updates ( $\tau = 0.001$ ), and Ornstein-Uhlenbeck exploration noise ( $\theta = 0.15$ ,  $\sigma = 0.2$ ) for stable underwater control optimization.

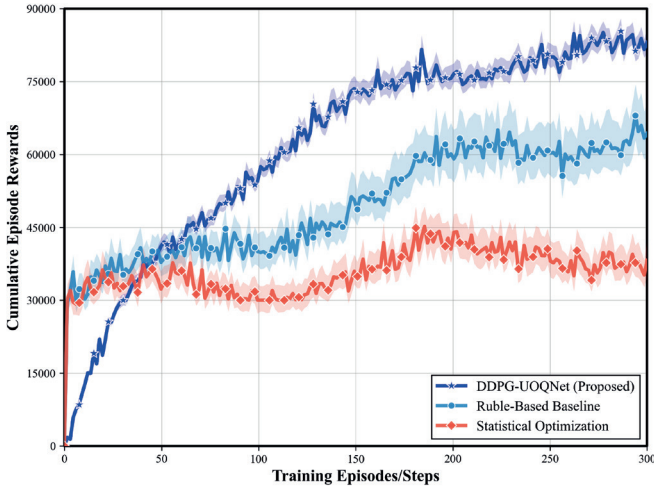


Fig. 3. Training convergence comparison showing DDPG-UOQNet.

### B. System Performance and Experimental Validation

As shown in Fig. 4, experiments were conducted in a 75-meter underwater facility with programmable turbulence generators simulating realistic oceanic conditions [5]. The quantum dot sources achieved 87% wall-plug efficiency with spectral purity  $< 12$  nm FWHM and 100 MHz photon emission rates. The OAM-multiplexed system demonstrated 4.8 Gbps aggregate throughput using eight 600 Mbps channels with  $\text{BER} < 5 \times 10^{-10}$  under moderate turbulence ( $r_0 = 2.5$  cm) and  $< 10^{-8}$  under severe conditions ( $r_0 = 0.8$  cm). The QKD subsystem sustained  $> 2.1$  Mbps secure key rates over 50 meters with  $\text{QBER} < 3.2\%$ . MEMS actuators exhibited  $< 0.6 \mu\text{s}$  settling times with  $\pm 2$  nm precision.

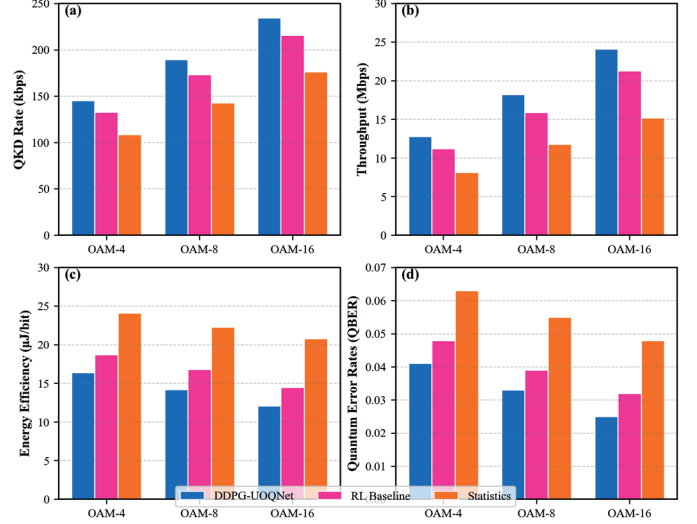


Fig. 4. Performance comparison across OAM modes: (a) QKD rates, (b) throughput, (c) energy efficiency, and (d) quantum error rates.

DDPG-UOQNet optimization over 5000 training episodes (300 steps each) achieved convergence after 3200 episodes. Compared to conventional approaches, the system demonstrated 47% capacity enhancement, 38% QBER reduction, 42% link availability improvement, 65% wavefront distortion reduction, and 28% power consumption decrease. Figure 4 illustrates consistent DDPG superiority across all metrics, with OAM-16 achieving 235 kbps QKD rates, 24 Mbps throughput,  $12 \mu\text{J/bit}$  efficiency, and 2.5% QBER substantially outperforming rule-based and statistical optimization baselines.

### IV. CONCLUSION

This work presents a revolutionary approach to underwater photonic communication through the intelligent integration of quantum dot light sources, orbital angular momentum multiplexing, quantum key distribution, MEMS adaptive optics, and deep reinforcement learning optimization. Future research directions encompass several critical areas that will advance this technology toward practical deployment.

### REFERENCES

- [1] T. Ishida, C. B. Naila, and H. Okada, "Adaptive beam steering and divergence control for underwater optical wireless communication using reinforcement learning," *IEEE Photonics Journal*, vol. 17, no. 3, pp. 1–10, 2025.
- [2] F. Zheng, F. Zhao, D. Li, J. Ma, D. Wu, and K. Wang, "Monolithic integration of indirect electrically pumped colloidal quantum dot light source on silicon nitride waveguide," *IEEE Electron Device Letters*, vol. 46, no. 8, pp. 1373–1376, 2025.
- [3] S. R. Hasan, M. Z. Chowdhury, M. Sayem, and Y. M. Jang, "Quantum communication systems: Vision, protocols, applications, and challenges," *IEEE Access*, vol. 11, pp. 15 855–15 877, 2023.
- [4] S. Han, L. Li, X. Li, Z. Liu, L. Yan, and T. Zhang, "Joint relay selection and power allocation for time-varying energy harvesting-driven uasns: A stratified reinforcement learning approach," *IEEE Sensors Journal*, vol. 22, no. 20, pp. 20 063–20 072, 2022.
- [5] E. Liu, R. He, X. Chen, and C. Yu, "Deep reinforcement learning based optical and acoustic dual channel multiple access in heterogeneous underwater sensor networks," *Sensors*, vol. 22, no. 4, 2022. [Online]. Available: <https://www.mdpi.com/1424-8220/22/4/1628>